NASA TECHNICAL MEMORANDUM

NASA TM X-71715

NASA TM X-71715

(NASA-TM-X-71715) V-GROOVED SILICON SOLAR CELLS (NASA) 10 p HC $3.25 CSCL 10B

N75-24119

Unclas

G3/44 22761

V-GROOVED SILICON SOLAR CELLS

by Cosmo R. Baraona and Henry W. Brandhorst
Lewis Research Center
Cleveland, Ohio 44135

TECHNICAL PAPER to be presented at
Eleventh Photovoltaic Specialists Conference
sponsored by the Institute of Electrical and
Electronics Engineers
Phoenix, Arizona, May 6-8, 1975

V-GROOVED SILICON SOLAR CELLS

Cosmo R. Baraona and Henry W. Brandhorst
Lewis Research Center
National Aeronautics and Space Administration
Cleveland, Ohio

E-8336

Abstract and Summary

Silicon solar cells with macroscopic V-shaped grooves and microscopically texturized surfaces have been made by preferential etching techniques. Various conditions for potassium hydroxide and hydrazine hydrate etching were investigated. Optical reflection losses from these surface were reduced. The reduced reflection occurred at all wavelengths and resulted in improved short circuit current and spectral response. Improved collection efficiency is also expected from this structure due to generation of carriers closer to the cell junction. Microscopic point measurements of collected current using a scanning electron microscope showed that current collected at the peaks of the texturized surface were only 80% of those collected in the valleys.

Introduction

In order to achieve maximum solar cell efficiency, reflectivity of the silicon surface must be reduced to as low a level as possible. This permits the maximum number of photons to enter the cell and contribute to the current. Use of single layer dielectric antireflection (AR, coatings has reduced the average reflectivity from about 35% to about 10%. The use of multilayer AR coatings can reduce the average silicon reflectivity to about 7%. However, this probably represents a practical limit for these AR coatings. To reduce reflection further other methods must be used.

The concept of reducing silicon reflectivity by physically altering the geometry of the silicon surface was introduced by Dale and Rudenberg.[1] In this approach numerous inverted tetrahedra were ultrasonically cut into the silicon surface. Reflectivity of this surface was reduced to about 4% as a result of multiple reflections from the silicon surface. This approach was abandoned because of difficulties and costs associated with the ultrasonic cutting process.

Recent work[2,3] has shown that preferential chemical etches on (100) orientation silicon surfaces can selectively expose (111) planes which intersect the surface with fourfold symmetry and form an angle of 54.7° between them. This geometry is useful in making a low reflection surface because incident light undergoes two reflections prior to escape. The geometry and angles of these structures, hence the reflectivity is dictated by the crystallography of the silicon.

The purpose of this paper is to report on chemical processes for obtaining grooved and pyramidally texturized silicon surfaces which lead to minimum reflectivity. Two types of etchants were used, KOH and hydrazine hydrate. Results of surface reflectivity measurements and cell performance tests will be described.

Optical Considerations

Several types of surface geometries can be envisioned for reducing reflectivity by multiple reflections from the silicon surface. The simplest is V-grooved as shown in Figure 1a. The surface of this structure consists of a series of parallel grooves which are V-shaped in cross section separated by flat sections of variable area. From crystallographic considerations the wall angle is about 55° to the horizontal and groove depth is 0.7 times groove width. Light incident on the flat spots between the grooves in Figure 1a is lost after a single reflection. However, light incident on a groove wall will be reflected into the adjacent groove wall where it has a second chance to be transmitted. Thus, if at a given wavelength there is a 0.3 reflection loss on a flat surface, a grooved surface will have a reflectivity of 0.09. Note that this reflection reduction is essentially independent of the wavelength of the incident light.

A second benefit provided by these macroscopically groved surfaces is improved carrier collection. Light entering a groove wall is refracted laterally in the cell. The path of the blue light is approximately 43° from the horizontal and that of the red light is about 48°. Thus absorption and carrier generation occurs closer to the junction and collection efficiency is improved. Furthermore the light paths are such that total internal reflection should occur if the rear face is smooth. Such reflection would lead to further enhancement of the red response and would be especially important in thin cells.

Two other classes of low reflection surface structures are shown in Figure 1. Figure 1b is a grid type pattern with perpendicularly intersecting V channels resulting in regularly spaced four sided-pyramids with either pointed or truncated tops. Figure 1c shows a series of randomly spaced and randomly sized pointed pyramids - a texturized surface. In all cases, the light reflected from the angled walls can undergo about two reflections prior to escaping from the surface. This leads to a minimum bare surface reflectivity of about 10%. Addition of an AR coating will reduce reflection even further.

Experimental Procedure

There are several preferential chemical etches that may be used for making low reflection surfaces. The best known is a potassium hydroxide (KOH) etch on (100) orientation silicon as reported by Stoller.[2] To make V-grooved samples, the silicon was first oxidized with steam to form a 0.2 μm thick SiO_2 layer. Parallel channels were opened in the oxide layer using photoresist techniques. Channel width was about 200 μm separated by about 140 μm wide oxide covered silicon. KOH-water compositions ranging from 3% to 50% by weight were used to form the grooves. Etch solution temperature was varied from 70 to 90° C and times from minutes to several hours were used.

Groove width (and hence depth) can be controlled by the width of the channel opened in the oxide. The flat regions between grooves can be eliminated by sizing the mask so that complete undercutting of the oxide occurs at the same time the bottom of the grooves is etched to completion. The size and spacing of the grooves is limited by available photoresist technology. Although groove sizes of the order of micrometers can be produced by this technology this option was not explored.

To avoid the difficulties of photomasks with microscopic dimensions these KOH etch conditions were also tried on unmasked silicon in an attempt to produce a texturized surface. The range of conditions tried (3%-50% KOH at 70 to 90° C) did not result in texturized surfaces. The surfaces which resulted were shinny and consisted of numerous square, shallow depressions.

A second preferential etch, hydrazine hydrate (HH), has been reported by Lee.[3]

He used this HH etch with oxide and photoresist masking as an isolation technique in integrated circuits. As in the previous case this etch was tried on (100) silicon without oxide masking. Both saw cut and polished surfaces were used. A range of HH and water (H_2O) compositions from 100% HH to 10% HH - 90% H_2O by volume was tried. Etch temperature ranged from 25° C to 115° C. Etch times were from a few seconds to 3 days. Many combinations of composition, time and temperature resulted in low reflectivity black velvet-like textured surfaces. Etch conditions most commonly used were 60% HH to 40% H_2O at 110° C for 10 minutes.

Both grooved and velvet surface wafers were made into solar cells using conventional cell fabrication steps. The NP junctions were formed using phosphorus oxychloride ($POCl_3$) diffusions in oxygen carrier gas at temperatures between 875 and 825° C for 30 minutes. Silver-only[4] and aluminum-silver non-back surface field (non-BSF) type contacts were applied. Evaporated tantalum oxide (Ta_2O_5) AR coatings .055 to .06 μm in thickness were used in some cases.

The scanning electron microscope (SEM) was used to view the surfaces produced. Also, when operated in the diode response mode, the SEM was used to map the microscopic photovoltaic response of junctions diffused in texturized surfaces. In this mode the scanning electron beam generates carriers over a microscopic area of the cell surface. These carriers are collected by the junction and amplified in an external circuit. This current is used to modulate an imaging screen to produce a picture of the surface which is related to the current collected from point to point on the cell surface.

Results and Discussions

Surface Texture

The near boiling KOH-water mixture used here with oxide masking and photoresist fabrication methods resulted in grooved and gridded surfaces (Figs. 1a and 1b). The walls of these grooves are (111) planes. From crystallographic considerations the wall angle is about 55° and the groove depth is about 0.7 times the width. The spacing between groove (i.e., the width of the flat spots) and the size or width of the grooves was controlled by the photomask spacing. The parallel grooves in the samples and solar cells made for this study were macroscopic in size - on the order of a hundred micrometers in width. A cross-sectional SEM photo of a grooved sample is shown in Figure 2a.

The KOH etch of unmasked (100) silicon resulted in a shiny surface consisting of numerous square, shallow depressions, shown in Figure 2b, ineffective for reducing reflection.

Views at 1800X magnification of a hydrazine-etched velvet surface from various angles are shown in Figure 3. Figure 3a is a scanning electron micrograph (SEM) of a portion of the sample viewed in the direction perpendicular to the sample surface. Figure 3b is another portion of the surface viewed from a 45° angle to the sample surface. Figure 3c is a view about 72° from the perpendicular and rotated about 40° compared with the view in Figure 3b. The varied viewing angles result in different surface appearance. It is clear that this velvet or textured surface consists of randomly spaced four sided, pointed tetrahedra. The photos show that the pyramids vary in dimensions with a maximum size and height of about 15 μm. Other textured surfaces with a differing range of tetrahedron size have also been made.

The development of the textured or velvet surface as a function of hydrazine etching time is shown in Figure 4. These are SEM photos taken at 1800X magnification and at a 45° viewing angle with zero rotation, i.e., looking directly at one face of the pyramids. The original highly damaged, structureless silicon surface is shown in Figure 4a. After one minute of etching with an approximate 50% HH-H_2O boiling etch, the tetrahedra emerge as small lumps separated by some flat spots. As etching continues the size and structural perfection of the tetrahedra increases. After 15 minutes (Fig. 4d) the flat spots disapear; only (111) planes are exposed and the etch rate slows.

For a given etch composition and temperature there appears to be an optimum etch time to achieve maximum structural perfection and uniformity. If etching continues beyond this time the pyramids begin to disappear and flat shiny regions similar to the nonmasked KOH etched samples previously described (Fig. 2b) begin to emerge. These nonuniformly etched regions are also influenced by the pre-etch surface condition of the silicon samples. Results indicate that a saw cut or lapped starting surface yields more uniformly texturized surfaces more consistently than chemically or mechanically polished starting surfaces. In all cases, of course, the starting surfaces must be clean.

Tetrahedron size can be decreased by controlling etch conditions. For example, a room temperature, 100% HH etch for several days gives a textured surface with a maximum pyramid size of about 5 μm. The structural perfection of such surfaces in some cases was degraded, i.e., flat shiny spots as described above were present. However the size of the pyramids obtained in this study should not affect the reflectivity and did not result in any known effect on cell fabrication.

Surface Reflectivity

Figure 5 shows the measured total reflectivity against wavelength of the incident light for several kinds of samples. The top curve is for a mirror-like mechanically polished silicon surface. The next two are for parallel grooved samples with differing amounts of surface area covered by grooves. This was accomplished by varying the groove spacing, so that the measured groove area expressed in percent was 16% and 36%, respectively. The total reflectivity at a given wavelength (R_T) for a parallel grooved surface is described by the following relation:

$$R_T = A_F R_F + A_G R_F^{2.1}$$

where A_F and A_G are the areas of the flats and grooves respectively and R_F is the reflectivity of the flats. The 2.1 exponent is based on an estimate that most photons incident on a groove undergo two reflections but a few undergo three so that overall about 2.1 reflections are achieved. Thus a simple equation can be used to calculate the reflectivities of the 16% and 36% grooved samples in Figure 5. The velvet surface in Figure 5 corresponds to a near 100% grooved surface. The bottom curve is for a velvet texturized surface with an antireflection coating and encapsulated in FEP teflon film. The reflectivity is low (4-5%) and relatively independent of wavelength. Samples with 100% grooved or texturized surfaces have a matte or velvet black appearance thus confirming the low reflection from textured surfaces.

In Figure 6 the reflectivity as a function of hydrazine etch time is shown. The major reflectivity decrease occurs in the first few minutes.

Cell Performance

Cells made from grooved or texturized surfaces have conventional characteristics when properly made. An I-V curve of a cell made on a texturized surface is shown in Figure 7. Normal open circuit voltage (V_{oc}) of .55 volts for 10 ohm-cm material has been attained. Low contact resistance (0.15 ohms) using non-BSF cells with 10 or 18 grid finger contact grid patterns have also been attained. The I-V curves of texturized cells made to date show fill factors between 68 and 72% and efficiencies between 11 and 12%. These results indicate that the texturized or grooved surface does not adversely effect the cell.

The low reflection of these surfaces results in improved short circuit current (I_{sc}). Air mass zero I_{sc}'s of 165 mA have been attained from 2x2 cells with deep (0.25 micrometer) junctions and non-optimized blue shifted AR coatings (i.e., greatest I_{sc} improvement after coating in the blue portion of the spectrum).

The spectral response of such a cell, shown in Figure 8, is equivalent to that of a comparably coated planar cell with a comparable junction depth. Attempts thus far to increase the current with shallower junctions in the texturized surface resulted in poor contact resistances, low V_{oc} and poor curve shapes.

Microscopic patterns of photovoltaic response of junctions diffused in the textured surface have been measured and one case is illustrated in Figure 9.

A normal incidence SEM view of a solar cell surface at 1950X magnification is shown in Figure 9a. The usual peaks (light areas) and valleys (dark regions) for a series of intermeshed pyramids are clearly visible. Figure 9b shows the same area with the SEM operated in a diode response or photovoltaic (PV) mode. Dark regions correspond to areas of low-junction collection while the light areas indicate higher response or collected current.

Comparison of Figures 9a and 9b shows that the peaks and edges of each pyramid are regions of lower response. A quantitative measure of the difference in response was obtained by scanning the SEM beam across a single line (connecting the arrows in Fig. 9a and b) and displaying the collected diode current as a function of distance. These results are shown in Figure 9c. Once again the peaks of the tetrahedra are areas of lower response and the valleys and edges have higher response. In these examples the pyramid peaks have 80% of the response of the valleys. This effect may be caused by multidirectional dopant penetration near the peaks and edges of the pyramids. At the top of the peaks phosphorus dopant from the $POCl_3$ source can enter the silicon lattice from each of the four faces of the pyramid while at the edges two sided diffusion is possible. Thus the dark low response regions in Figure 9b may be dopant saturated, degenerate dead regions with poor material properties which then results in poor junction collection in these regions. Conversely, the valleys may be areas of low dopant penetration but have higher response than the peaks. If this explanation is correct, the overall implication may be that a starved source type of diffusion may be desirable for textured surfaces and a balance between peak region overdoping and valley region underdoping will have to be found. Thus, it is probable that textured cell efficiencies can be increased by [illegible] junction fabrication to achieve shallower junctions with optimized dopant profiles having no dead regions.

Enhancement of collection efficiency has been seen in radiation damaged cells. A solar cell with 65% macroscopic parallel grooving was irradiated with one MeV electrons. Figure 10 shows the decrease in effective diffusion length, a measure of collection efficiency, with one MeV electron fluence for the 10 ohm-cm grooved cell and a conventional, smooth 10 ohm-cm cell.

Presumably the true diffusion length in both cells changed the same amount with irradiation but the collection of carriers was not impaired as quickly in the grooved cell. The macroscopically grooved cell therefore exhibits a lower damage coefficient.

Conclusions

Several methods of making different types of grooved silicon surfaces were demonstrated. Optical reflection was significantly reduced and can be approximately predicted using a simple formula. Hydrazine etched (100) silicon wafers resulted in texturized surfaces which exhibit a high degree of structurally perfect, pointed tetrahedra. Reflectivity is reduced most rapidly in the first few minutes of hydrazine etching time.

Solar cells made from grooved and texturized surfaces had normal voltages and fill factors and improved short circuit currents as expected. Efficiencies of 12% were obtained without optimization of processing conditions. Currents from the peaks of the pyramids on texturized surfaces were about 80% those of the valleys. Radiation damage results show that collection efficiency decreases less rapidly when solar cells are made with macroscopically grooved surfaces.

References

1. Dale, B. and Rudenberg, H. G., "Photovoltaic Conversion, 1. High Efficiency Silicon Solar Cells," Proceedings 14th Annual Power Sources Conf., U. S. Army Signal Research & Development Lab., Ft. Monmouth, New Jersey, May 17-19, 1960.

2. Stoller, A. I., "The Etching of Deep Vertical-Walled Patterns in Silicon," RCA Review, June 1970.

3. Lee, D. B , "Anisotropic Etching of Silicon," Journal of Applied Physics, Vol. 40, No. 11, October 1969.

4. Lamneck, John H., Jr., and Schwartz, Lawrence, "A Reliable All-Silver Front Contact for Silicon Solar Cells," NASA TM X-2544, May 1972.

E-8336

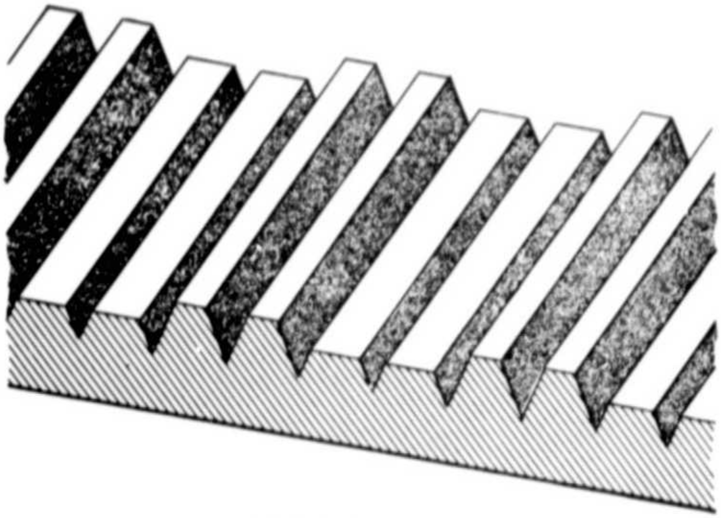

(a) PARALLEL GROOVED (SPACING CONTROLLABLE).

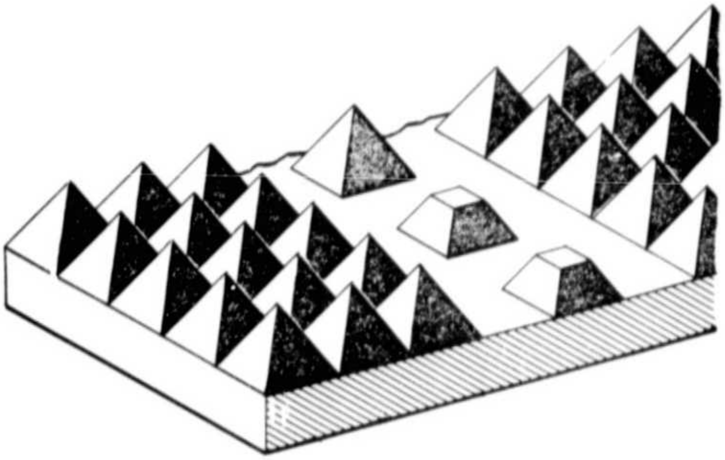

(b) UNIFORM GRID (EQUAL SIZE AND SPACING).

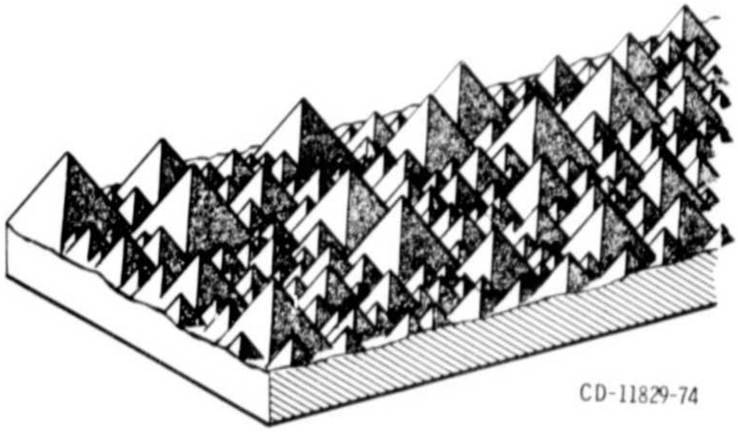

(c) TEXTURIZED (RANDOM SIZE AND SPACING).

Figure 1. - Classes of low reflection surfaces.

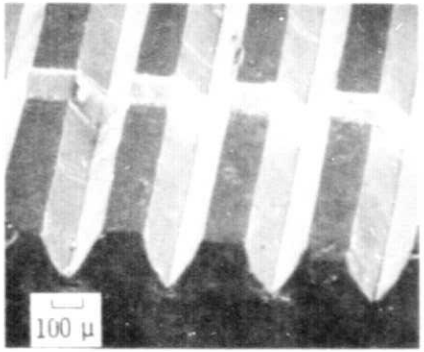

(a) CROSS SECTION OF PARALLEL GROOVES.

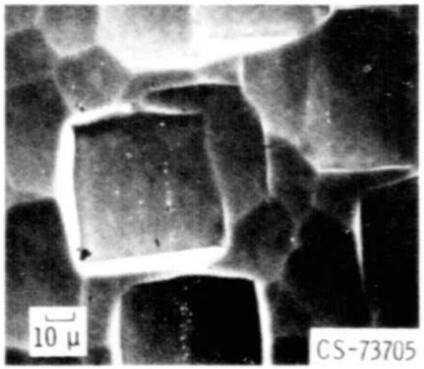

(b) UNMASKED KOH ETCHED SURFACE, NORMAL VIEWING ANGLE.

Figure 2. - KOH etched surfaces.

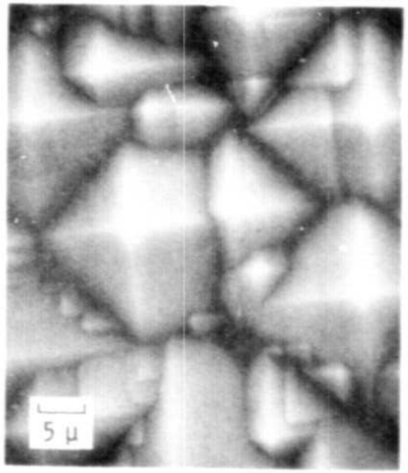

(a) PERPENDICULAR TO SAMPLE.

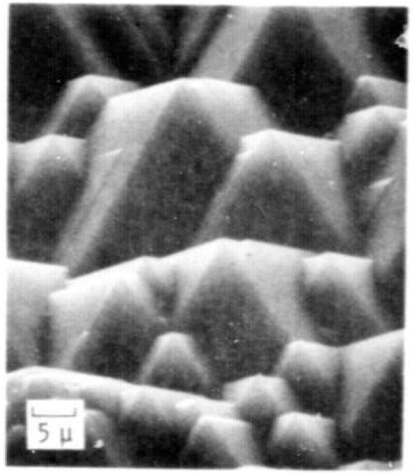

(b) 45^0 OBLIQUE VIEW.

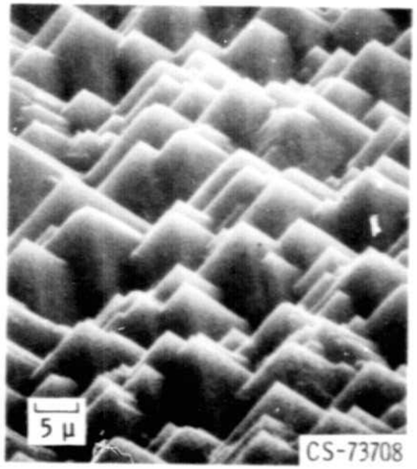

(c) 45^0 OBLIQUE VIEW ROTATED 70^0.

Figure 3. - Views of textured surfaces. X1800 magnification SEM photos.

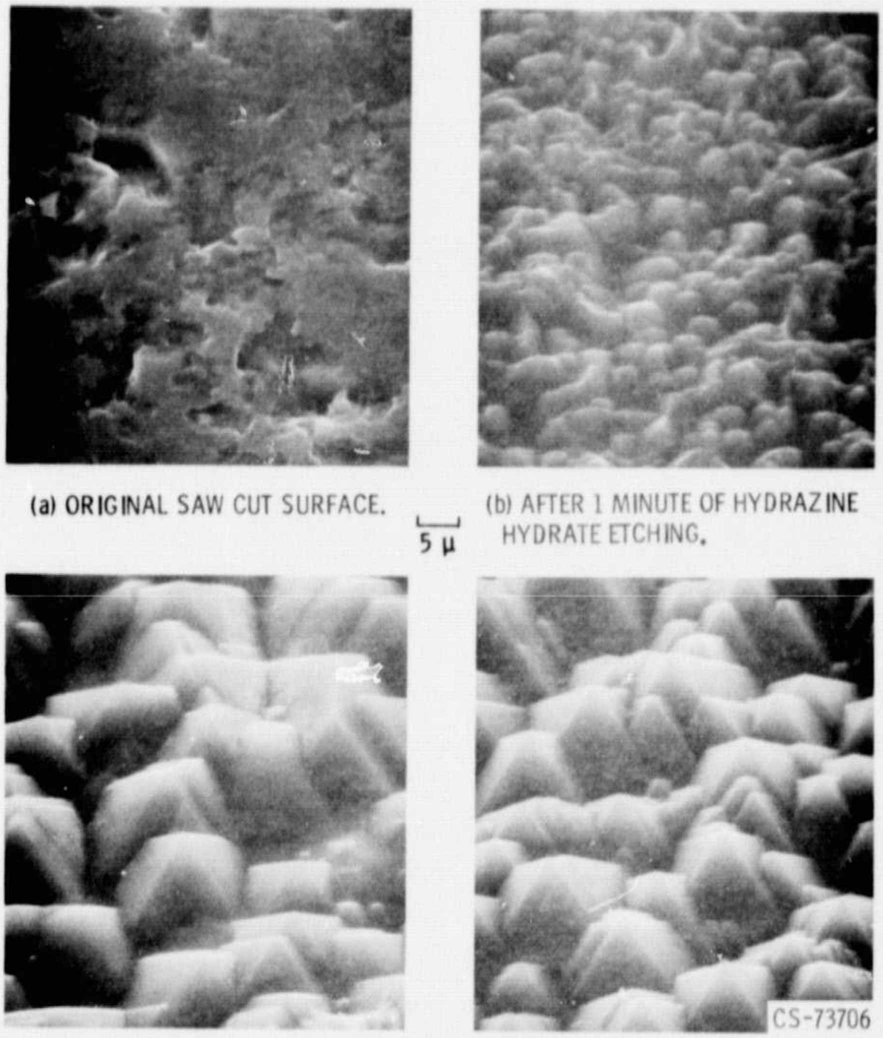

(a) ORIGINAL SAW CUT SURFACE.

(b) AFTER 1 MINUTE OF HYDRAZINE HYDRATE ETCHING.

(c) AFTER 6 MINUTES OF HYDRAZINE HYDRATE ETCHING.

(d) AFTER 15 MINUTES OF HYDRAZINE HYDRATE ETCHING.

Figure 4. - Development of texturized surface. X1800 magnification SEM photos.

E-8336

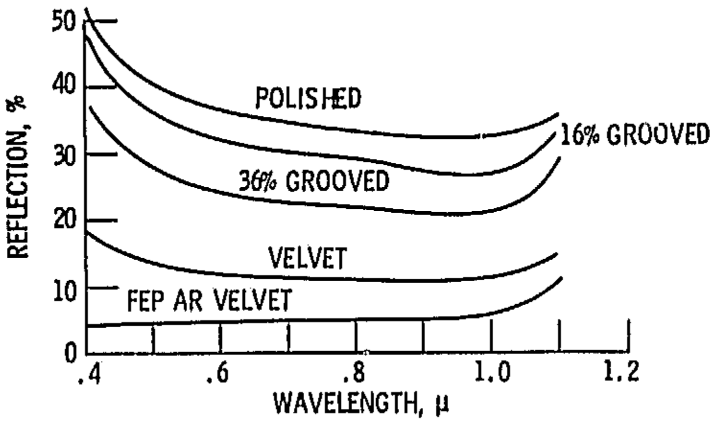

Figure 5. - Total reflection for various types of silicon surfaces.

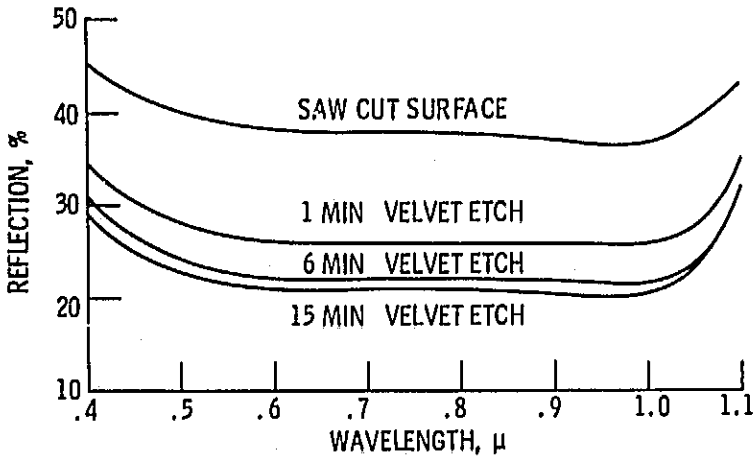

Figure 6. - Total reflection for various hydrazine etch times.

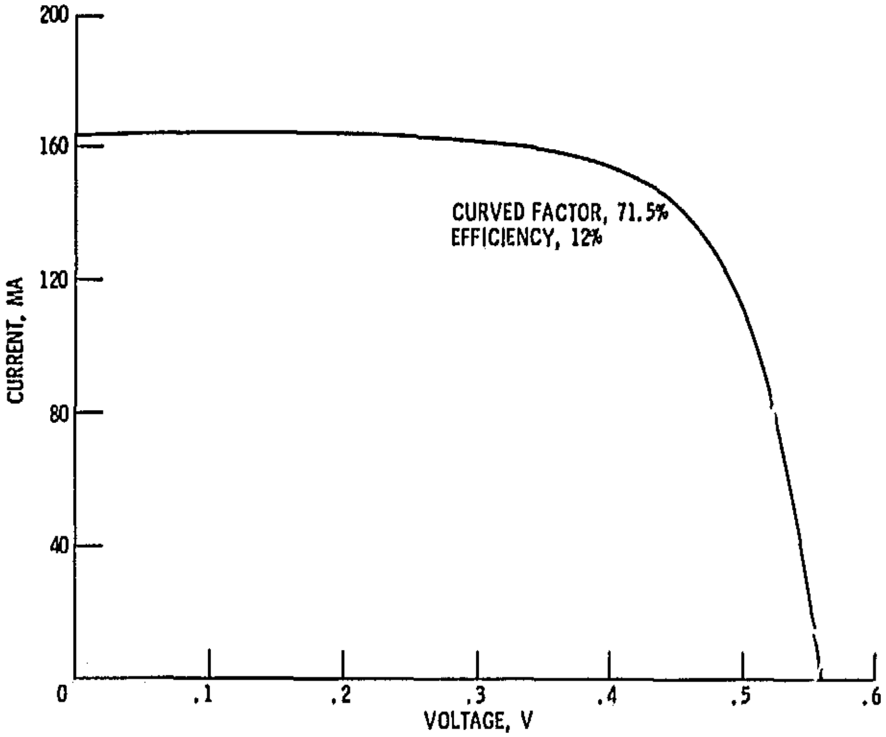

Figure 7. - Current voltage for texturized cell.

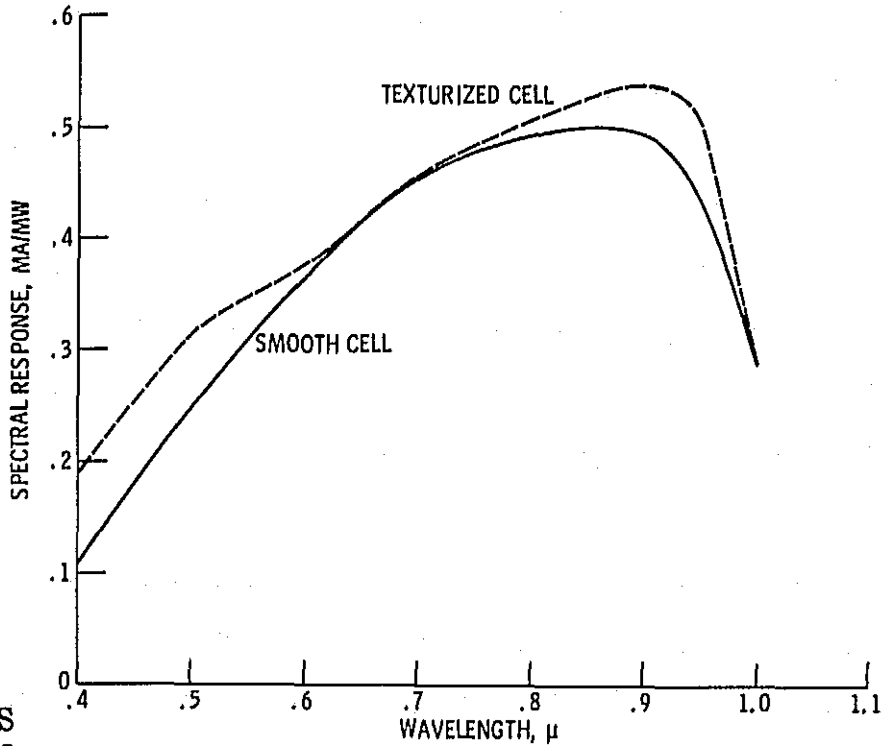

Figure 8. - Comparison of spectral response of texturized and conventional smooth surface solar cells with antireflection coatings.

NASA-Lewis

ORIGINAL PAGE IS
OF POOR QUALITY

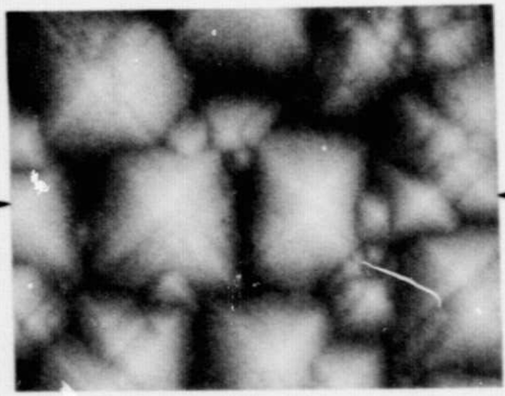

(a) SEM MODE; NORMAL VIEW AT X1950.

5 μ

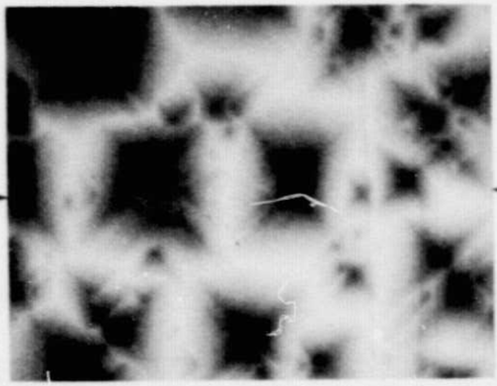

(b) PV MODE; NORMAL VIEW AT X1950.

(c) LINE SCAN ACROSS. CS-73707

Figure 9. - Diode response of texturized surface.

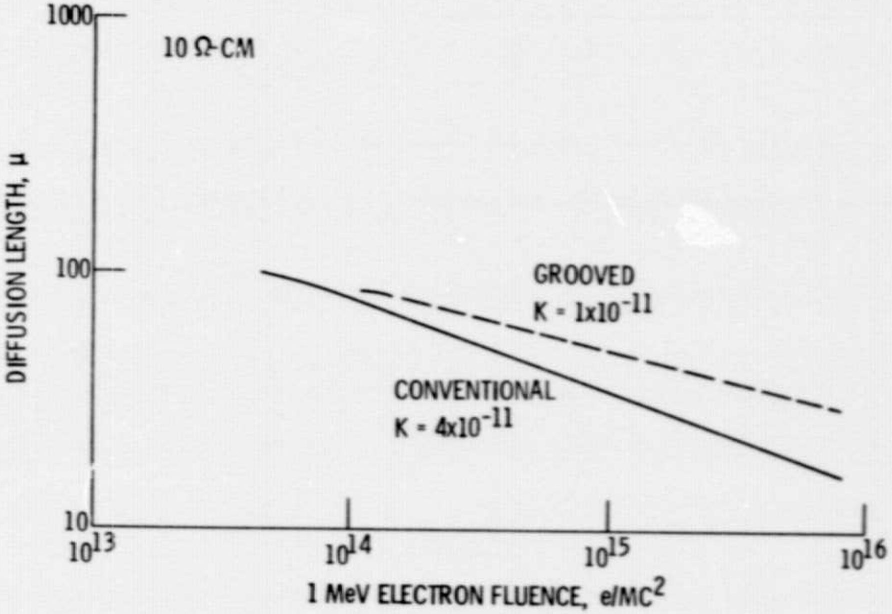

Figure 10. - Radiation damage of grooved solar cell.